Computing finite rotations of shells by an asymptotic-numerical method

Hamid Zahrouni, Bruno Cochelin, Michel Potier-Ferry

Computing finite rotations of shells by an asymptotic-numerical method

H. Zahrouni[a,*], B. Cochelin[b], M. Potier-Ferry[a]

[a]*Laboratoire de Physique et Mécanique des Matériaux, U.M.R. CNRS 7554, Institut Supérieur de Génie Mécanique et Productique, Université de Metz, Ile du Saulcy, 57045 Metz Cedex 01, France*

[b]*Laboratoire de Mécanique et Acoustique (UPR CNRS 7051) Ecole Supérieure de Mécanique de Marseille, I.M.T., Technopôle de Chateau Gombert, 13451 Marseille Cedex 20, France*

We present an asymptotic numerical algorithm for the computation of elastic shells with large rotations. The theoretical formulation involves a three-field Hu–Washizu functional, which allows us to put the problem into a quadratic framework. The spatial discretization is based on geometrically exact element, recently presented by Büchter et al. [Büchter et al., Three dimensional extension of non-linear shell formulation based on the enhanced assumed strain concept, Int. J. Numer. Methods Engrg. 37 (1994) 2551–1568]

Several classical benchmarks are discussed to define the best strategy and to assess the validity and the efficiency of the present method, as compared to more classical iterative algorithms.

1. Introduction

The Asymptotic Numerical Method (ANM) is a family of algorithms which solve nonlinear problems, associating asymptotic expansions with numerical discretization methods. Indeed, it allows us to seek solution branches in the shape of power series expansions with respect to a path parameter. In this way, we can transform the nonlinear problem into a set of recurrent, well-posed, linear problems which admit the same tangent operator. Then, these linear problems are solved numerically, generally by the Finite Element Method. Because the radius of convergence of such series is finite, a continuation technique has been proposed [15]: since the solution path is represented by a closed form formula, it is rather easy to define a range of validity of that representation, which defines the step length. So, the step length is computed a posteriori, which is not the case with incremental iterative methods. Thus, an adaptive step length is determined in a simple and optimal way, which is a key point as for efficiency and robustness of the ANM. Comparisons between the ANM and more classical algorithms can be forund for instance in [1,9,20,17]. In this paper, we apply the algorithm presented in [15] to large rotations of shell structures.

Historically, Thompson and Walker [32] were the first to compute many terms of series by the finite element method. This perturbation method has been associated with a reduced basis technique [24–26]. Nevertheless, pessimistic conclusions had been put forward several times about the numerical efficiency of these methods [29,18]. Recently, the reduced basis technique has been compared with the representation by power series [23] and in the present state, the second method with a large order of truncature seems to be better than the first one. To improve the efficiency of the method, it has been proposed to set the considered problem in a quadratic framework, i.e. in a form like

* Corresponding author.

$$R(U, \lambda) = L(U) + Q(U, U) - \lambda F = 0 \tag{1}$$

where U is the unknown vector field, λ is a scalar parameter, $L(.)$ is a linear operator and $Q(.,.)$ is a quadratic one [16,5,13]. Within such a framework, the computation time of the right-hand sides remains smaller than the one due to the treatment of the tangent matrix and therefore, a step of ANM requires about the same CPU time as one step with the modified Newton–Raphson method [5,13]. This quadratic framework is quite natural for the Navier–Stokes equations [20,33,12]. The ANM has been widely applied to nonlinear elastic shells with moderate rotations [5,13–15]: it is sufficient to consider the couple displacement–stress as the unknown U to put the Von Karman equations into a quadratic framework. More recently, the ANM has been adapted for the treatment of plastic materials with J2 deformation theory, of unilateral contact and of Norton–Hoff materials [9,17].

The aim of this paper is to extend the ANM for the computation of shells with large rotations. A possible way should be to keep the moderate rotations' framework, to use the up-dated Lagrangian scheme, but the step lengths should be limited by the range of validity of the Von Karman equations. So, it seems more attractive to apply one of the numerous shell models which allows large rotations in a total Lagrangian framework. Unfortunately, these models involve different methods of parametrization and most of them use a proper orthogonal tensor or an equivalent finite rotation vector. On this subject, we note the remarkable contribution of Argyris [2] and a number of works which has allowed one to solve many problems of structural mechanics when large rotations are considered [28,27,6,4,19,21]. In this context, the field equations cannot be written simply in a quadratic form. There were two recent attempts to solve this question by using an asymptotic-numerical algorithm. The first paper [7] proposes an approximation only and the range of validity remains limited. In the second one [1], the algorithm to compute the series is altered and many terms of the series can be obtained, which gives satisfactory results. We propose here another way, which does not require any modification of the standard asymptotic-numerical algorithm. The basic idea is to consider a shell model, whose kinematic is described by a mid-surface displacement only and by a director vector, which permits us to set the problem in the quadratic form (1). An efficient and geometrically exact element has been proposed by Büchter et al. [11] and we shall use it in the discretisation step of the algorithm.

2. A three-field variational formulation

The considered shell element is based on a three-dimensional formulation. In the present paper, we will limit ourselves to a linear elastic constitutive law, which restricts most practical applications to the small strain case, but allows for arbitrarily large rotations. The account of a nonlinear constitutive law will be presented in a forthcoming paper. The unknowns are the displacement field u, the Green–Lagrange strain γ and the second Piola–Kirchhoff stress tensors S. The equations of the problem are equivalent to the stationarity of the Hu–Washizu functional

$$\Pi_{\mathrm{HW}}(u, \gamma, S) = \int_v \frac{1}{2} ({}^t\gamma : D : \gamma) - {}^tS : (\gamma - Bu)\, \mathrm{d}v - \lambda P_e(u) \tag{2}$$

where D is the elastic stiffness tensor, $\lambda P_e(u)$ is the work done by the external load, λ is a scalar load parameter and Bu is the compatible strain which is a quadratic function of the displacement. The stationarity of the functional with respect to the three fields leads, respectively to the virtual work equation, to the constitutive equation and to the displacement–strain relationship $\gamma = Bu$.

In the present formulation, we consider a shell element proposed by Büchter et al. [11] with linear displacement variation across the thickness as in conventional shell formulations but which includes a linear varying thickness stretch as extra variable. This extra unknown permits to use a complete 3-D constitutive law without condensation and also large strain effects. It is incorporated via the Enhanced Assumed Strain (EAS) concept which has been introduced by Simo and Rifai [31] to improve the performance of displacement finite element. The principle consists in introducing an enhanced part of the strain $\tilde{\gamma}$, which does not depend on the displacement and which is required to be orthogonal to the stress field

$$\gamma - Bu = \tilde{\gamma}, \qquad \int_v ({}^tS : \tilde{\gamma})\, \mathrm{d}v = 0 \tag{3}$$

Hence, the stress field can be eliminated, allowing the reduction of the three-field functional to a two-field one, i.e. the displacements and the enhanced strains. The functional can now be written as follows:

$$\Pi_{\mathrm{EAS}}(u,\ \tilde{\gamma}) = \int_v \frac{1}{2}\ {}^t(Bu + \tilde{\gamma}) : D : (Bu + \tilde{\gamma})\ \mathrm{d}v - \lambda P_e(u) \tag{4}$$

Stationarity conditions associated with (4) produce the equilibrium equation and the compatibility equation which is equivalent to the orthogonality condition

$$\delta\Pi_{\mathrm{EAS}}(u,\ \tilde{\gamma}) = \int_v {}^t(\delta B\ u + \delta\tilde{\gamma}) : D : (Bu + \tilde{\gamma})\ \mathrm{d}v - \lambda P_e(\delta u) = 0 \tag{5}$$

The present three-dimensional formulation is not different from the initial problem, because the exact solution is $\tilde{\gamma} = 0$. The interest of the formulation (5) will appear, when the displacement field is assumed linearly varying across the thickness, as it is usual within the shell models. As is well known, such a displacement field is in contradiction with zero normal stress hypothesis, because it involves a vanishing thickness stretch. That is why the classical formulations condense the 3-D constitutive law and determine the thickness stretch by zero normal stress assumption. With the chosen element, the enhanced strain $\tilde{\gamma}$ is introduced in such a way that the normal stress vanishes approximately, which avoids condensing the 3-D constitutive law. Eq. (5) is the usual starting point for displacement element model, however, it is not the best formulation for applying a perturbation technique, since the equilibrium equation is cubic with respect to the displacement field u. The best numerical efficiency is obtained by using a quadratic framework, which can easily be achieved by reintroducing the stress field and the constitutive law as in [5,15].

This leads to the following equation with respect to the unknowns $(u, S, \tilde{\gamma})$

$$\int_v \left\{ {}^t\delta S : \left[(Bu + \tilde{\gamma}) - D^{-1} : S\right] + {}^tS : (\delta(Bu) + \delta\tilde{\gamma})\right\} \mathrm{d}v - \lambda P_e(\delta u) = 0 \tag{6}$$

In Eq. (6), one recognizes, first the virtual work equation and the compatibility one as in (5), second the constitutive equation

$$S = D : (Bu + \tilde{\gamma})$$

where the strain $(Bu = \gamma_l(u) + \gamma_{nl}(u, u))$ has been completed by the incompatible term $\tilde{\gamma}$.

Now, we can write Eq. (6) in the following simple form

$$R(U,\ \lambda) = L(U) + Q(U, U) - \lambda F = 0 \tag{7}$$

where

$$U = \begin{pmatrix} u \\ \tilde{\gamma} \\ S \end{pmatrix}$$

is a mixed unknown, $L(.)$ a linear operator, $Q(.,.)$ a quadratic one, F the external load vector, and R the residual vector.

$$\langle L(U), \delta U\rangle = \int_v \left\{ {}^t\delta S : \left[(\gamma_l(u) + \tilde{\gamma}) - D^{-1} : S\right] + {}^tS : (\gamma_l(\delta u) + \delta\tilde{\gamma})\right\} \mathrm{d}v$$

$$\langle Q(U, U), \delta U\rangle = \int_v \left\{ {}^t\delta S : \gamma_{nl}(u, u) + {}^tS : 2\gamma_{nl}(u, \delta u)\right\} \mathrm{d}v$$

$$\langle F, \delta U\rangle = P_e(\delta u)$$

The bilinear quadratic operator $Q(U_1, U_2)$ associated with the quadratic operator $Q(U, U)$ is given by:

$$\langle Q(U_1, U_2), \delta U\rangle = \int_v \left\{ {}^tS_1 : \gamma_{nl}(u_2, \delta u) + {}^tS_2 : \gamma_{nl}(u_1, \delta u) + {}^t\delta S : \gamma_{nl}(u_1, u_2)\right\} \mathrm{d}v$$

We want to insist on the fact that the motivation for introducing the stress field and the constitutive law is to write the full problem under the very simple quadratic form (7) which is well suited for asymptotic expansions. We have no intention to use a mixed finite element in the following.

3. An asymptotic numerical algorithm

We propose in this section, to solve the nonlinear problem (7) by a similar method as in the moderate rotation case, see for instance [14,15]. At first, we apply perturbation techniques which allow us to transform the nonlinear problem into a sequence of linear ones. When these latters are established until a given order p, we proceed to condense the stress field in order to use a classical displacement finite element. Then, the resulting continuous problems are discretized and solved by finite element method. As all these problems have the same tangent operator, we analytically obtain a part of the solution path with only one stiffness matrix decomposition. A continuation procedure is proposed to describe the whole solution branch.

3.1. Perturbation technique

This method consists in searching the solution path of the problem under an asymptotic expansion form, in the neighbourhood of a known solution (U_0, λ_0), with respect to a path parameter. This latter will be defined subsequently. Now, if we introduce these developments in problem equations, we obtain a recurrent set of linear problems which have the same tangent operator. In the present formulation, the mixed vector U and the load parameter λ are expanded into power series of a path parameter 'a', whom we take as the projection of the pair $(u - u_0, \lambda - \lambda_0)$ on the tangent direction (u_1, λ_1)

$$U(a) = U_0 + aU_1 + a^2U_2 + \cdots = \begin{pmatrix} u_0 \\ \tilde{\gamma}_0 \\ S_0 \end{pmatrix} + a\begin{pmatrix} u_1 \\ \tilde{\gamma}_1 \\ S_1 \end{pmatrix} + a^2\begin{pmatrix} u_2 \\ \tilde{\gamma}_2 \\ S_2 \end{pmatrix} + \cdots \tag{8}$$

$$\lambda(a) = \lambda_0 + a\lambda_1 + a^2\lambda_2 + a^3\lambda_3 + \cdots \tag{9}$$

$$a = \langle u - u_0, u_1 \rangle + (\lambda - \lambda_0)\lambda_1 \tag{10}$$

Now, by substituting Eqs. (8) and (9) into Eqs. (7) and (10), and equating like powers of 'a', we obtain a sequence of linear problems at different orders

order 1:

$$\begin{aligned} &L_t(U_1) = \lambda_1 F \\ &\langle u_1, u_1 \rangle + \lambda_1^2 = 1 \end{aligned} \tag{11}$$

order 2:

$$\begin{aligned} &L_t(U_2) = \lambda_2 F - Q(U_1, U_1) \\ &\langle u_2, u_1 \rangle + \lambda_2\lambda_1 = 0 \end{aligned} \tag{12}$$

order p:

$$\begin{aligned} &L_t(U_p) = \lambda_p F - \sum_{r=1}^{p-1} Q(U_r, U_{p-r}) \\ &\langle u_p, u_1 \rangle + \lambda_p\lambda_1 = 0 \end{aligned} \tag{13}$$

The tangent operator is denoted by $L_t(.) = L(.) + 2Q(U_0,.)$ and it depends on the initial solution only.

At order p, the problem is formulated as

Find the parameter λ_p and the mixed vector $U_p \begin{pmatrix} u_p \\ \tilde{\gamma}_p \\ S_p \end{pmatrix}$

which verify:

$$L_t(U_p) = \lambda_p F - \sum_{r=1}^{p-1} Q(U_r, U_{p-r})$$

$$\langle u_p, u_1 \rangle + \lambda_p \lambda_1 = 0$$

3.2. Condensation of the stresses

Let us now rewrite in detail the linear problem at order p in terms of u_p, $\tilde{\gamma}_p$, S_p. With the notation we have introduced, we obtain

$$\int_v \left\{ {}^t\delta S : \left[\left(\gamma_l(u_p) + \tilde{\gamma}_p \right) - D^{-1} : S_p \right] + {}^tS_p : (\delta\tilde{\gamma} + \gamma_l(\delta u)) \right\} dv$$

$$+ \int_v \left\{ {}^t\delta S : 2\gamma_{nl}(u_0, u_p) + {}^tS_0 : 2\gamma_{nl}(u_p, \delta u) + {}^tS_p : 2\gamma_{nl}(u_0, \delta u) \right\} dv$$

$$= \langle \lambda_p F, \delta u \rangle - \int_v \left\{ \sum_{r=1}^{p-1} {}^t\delta S : \gamma_{nl}(u_r, u_{p-r}) + \sum_{r=1}^{p-1} {}^tS_r : 2\gamma_{nl}(u_{p-r}, \delta u) \right\} dv \tag{14}$$

Eq. (14) is equivalent to the following equilibrium equation (15), constitutive law (16) and compatibility equation (17).

$$\int_v \left\{ {}^tS_p : [\gamma_l(\delta u) + 2\gamma_{nl}(u_0, \delta u)] + {}^tS_0 : 2\gamma_{nl}(u_p, \delta u) \right\} dv = \langle \lambda_p F, \delta u \rangle - \int_v \left\{ \sum_{r=1}^{p-1} {}^tS_r : 2\gamma_{nl}(u_{p-r}, \delta u) \right\} dv \tag{15}$$

$$S_p = D : \left[\gamma_l(u_p) + 2\gamma_{nl}(u_0, u_p) + \tilde{\gamma}_p + \sum_{r=1}^{p-1} \gamma_{nl}(u_r, u_{p-r}) \right] \tag{16}$$

$$\int_v {}^tS_p : \delta\tilde{\gamma} \, dv = 0 \tag{17}$$

With a view to apply a finite element method where only u and $\tilde{\gamma}$ are interpolated, we substitute (16) into (15) and (17). Thus, we obtain two equations representing the equilibrium and compatibility conditions in terms of u_p, $\tilde{\gamma}_p$

$$\int_v \left\{ {}^t\left[\gamma_l(u_p) + 2\gamma_{nl}(u_0, u_p) + \tilde{\gamma}_p \right] : D : [\gamma_l(\delta u) + 2\gamma_{nl}(u_0, \delta u)] \right.$$

$$\left. + {}^tS_0 : 2\gamma_{nl}(u_p, \delta u) \right\} dv = \langle \lambda_p F, \delta u \rangle - \int_v \sum_{r=1}^{p-1} {}^tS_r : 2\gamma_{nl}(u_{p-r}, \delta u) \, dv$$

$$+ \int_v \sum_{r=1}^{p-1} {}^t\gamma_{nl}(u_r, u_{p-r}) : D : [\gamma_l(\delta u) + 2\gamma_{nl}(u_0, \delta u)] \, dv \tag{18}$$

$$\int_v {}^t\left[\gamma_l(u_p) + 2\gamma_{nl}(u_0, u_p) + \tilde{\gamma}_p \right] : D : \delta\tilde{\gamma} \, dv = - \int_v \sum_{r=1}^{p-1} {}^t\gamma_{nl}(u_r, u_{p-r}) : D : \delta\tilde{\gamma} \, dv \tag{19}$$

Eqs. (18), (19) and (16) are equivalent to (14). Now we turn to the presentation of the element and the discretization of (18) and (19).

3.3. Finite element discretization

In this section, Eqs. (18) and (19) are discretized with the help of a geometrically exact shell element, proposed by Büchter et al. [11]. The unknowns are the mid-surface displacement and its director vector. As the geometry of the shell is treated exactly, this formulation takes into account the quadratic terms in membrane and flexural deformation. Furthermore, it is based on the classical shell theories which consider a linearly varying displacement field in thickness direction; but, this model enriches its six parameter theory via the EAS proposed by Simo and Rifai [31] by introducing an additional deformation which is linear in thickness direction. This new parameter will allow us to use a complete three-dimensional constitutive law, allowing large strain effects and avoiding locking phenomena. For this parameter, no inter-element continuity is required; so, it can be eliminated by condensation on the element level.

Geometry and kinematic of the proposed shell element are described in Fig. 1. The position vector x of undeformed shell is defined by mid-surface vector r and its director vector a_3

$$x(\theta^1,\theta^2,\theta^3) = r(\theta^1,\theta^2) + \theta^3 a_3(\theta^1,\theta^2) \tag{20}$$

By using the assumption of a linearly varying displacement field in thickness direction, this latter can be written in the following form

$$u(\theta^1, \theta^2, \theta^3) = v(\theta^1, \theta^2) + \theta^3 w(\theta^1, \theta^2) \tag{21}$$

in which v represents the displacement of the mid-surface and w is the difference vector between the undeformed and deformed directors.

The fields v and w are interpolated via the shape functions of the classical eight node serendipity quadrilateral. By collecting the nodal values of v and w in the vector q, the displacements u, its virtual counterpart δu and its gradient $\theta(u)$ are linked to q and δq as follows [35]

$$\{u\} = [N]\{q\} \qquad \{\delta u\} = [N]\{\delta q\} \qquad \{\theta(u)\} = [G]\{q\} \tag{22}$$

where $[N]$ is the matrix of shape functions and $[G]$ is their gradient matrix.

The Green–Lagrange strain which is the nonlinear compatible strain can be expressed in covariant base in the following form

$$\gamma_{ij}(u) = \frac{1}{2}\left(\frac{\partial u}{\partial \theta^i}\, g_j + \frac{\partial u}{\partial \theta^j}\, g_i + \frac{\partial u}{\partial \theta^i}\frac{\partial u}{\partial \theta^j}\right) \tag{23}$$

where g_i are covariant base vectors. The strain $\gamma(u)$ can be written in matricial form as

$$\{\gamma(u)\} = \{\gamma^l + \gamma^{nl}\} = \left([R] + \frac{1}{2}[A(q)]\right)[G]\{q\} \tag{24}$$

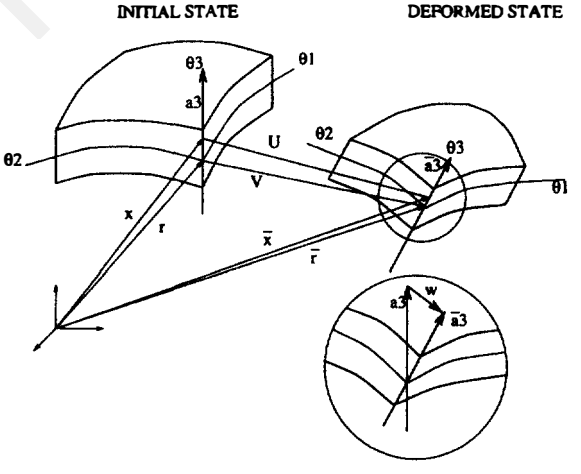

Fig. 1. Shell geometry and kinematic.

$$\{\delta\gamma(u)\} = \{\delta\gamma^{1}\} + \{\delta\gamma^{nl}\} = [\bar{B}(q)]\{\delta q\} = \left([R] + \frac{1}{2}[A(q)]\right)[G]\{\delta q\} \tag{25}$$

where $[R]$, $[A(q)]$, $[G]$, $\{q\}$ relate, respectively, to covariant base components matrix, displacement gradient matrix, gradient of shape functions matrix and nodal displacement vector. These formula are exactly the same as in [15] and [35]), except for the matrix $[R]$ which is due to the non orthogonal base considered in this formulation. This matrix is given in appendix A.

The additional strain $\tilde{\gamma}$ is chosen to be linearly varying in thickness direction

$$\tilde{\gamma} = \theta^{3}\,\tilde{\beta}_{33}(\theta^{1}, \theta^{2}) g^{3} \otimes g^{3} \tag{26}$$

and for the strain component $\tilde{\beta}_{33}$ no interelement continuity is required. A bilinear polynomial is assumed for $\tilde{\beta}_{33}$

$$\tilde{\beta}_{33} = \alpha_1 + \alpha_2 \xi + \alpha_3 \eta + \alpha_4 \xi\eta \tag{27}$$

$$\{\tilde{\gamma}_{33}\} = [B_\alpha][\alpha] \tag{28}$$

where ξ, η are the standard element co-ordinates. The extra-unknown parameters α_1, α_2, α_3, α_4 can be eliminated on the element level (see [11]).

We can rewrite the constitutive equation (16) in matricial form

$$\{S_p\} = [D]\left\{[\bar{B}(q_0)]\{q_p\} + [B_\alpha]\{\alpha_p\} + \sum_{r=1}^{p-1} \frac{1}{2}[A(q_r)]\{\theta(q_{p-r})\}\right\} \tag{29}$$

After discretization, Eq. (19) is solved on the element level giving then the parameters α_p in terms of the nodal variables q_p

$$\{\alpha_p\} = [K_{\alpha\alpha}^{-1}]([R_p^{\alpha}] - [K_{\alpha u}]\{q_p\}) \tag{30}$$

By substituting Eq. (30) into (18), we obtain, after discretization and assembling, the following form which represents the equilibrium of the global structure

$$[K_T]\{q_p\} = \lambda_p\{F\} + \mathop{\wedge}_{e=1}^{NbElm} (\{F_p^{nl}\} - [K_{u\alpha}][K_{\alpha\alpha}^{-1}]\{R_p^{\alpha}\}) \tag{31}$$

where K_T denotes the tangent stiffness matrix, $\wedge$ standard assembly operator, *NbElm* element number of the discretized structure, F is the external load vector and λ_p the scalar load parameter at order p.

$$K_T = \mathop{\wedge}_{e=1}^{NbElm} [(K_{uu} + K_\sigma) - {}^{t}K_{\alpha u}K_{\alpha\alpha}K_{\alpha u}]$$

$$K_{uu} = \int_v {}^{t}[\bar{B}][D][\bar{B}]\,dv \qquad K_\sigma = \int_v {}^{t}[G][\tilde{S}_\bullet][G]\,dv$$

$$K_{\alpha u} = \int_v {}^{t}[\bar{B}]\,[D][B_\alpha]\,dv \qquad K_{\alpha\alpha} = \int_v {}^{t}[B_\alpha][D][B_\alpha]\,dv$$

The classical right-hand sides within asymptotic numerical method are denoted by $\{F_p^{nl}\}$ and $\{R_p^{\alpha}\}$, which depend on solutions at the previous $p-1$ orders and expressed as follows:

$$\{F_p^{nl}\} = -\int_v {}^{t}[G] \sum_{r=1}^{p-1} \frac{1}{2} {}^{t}[A(q_{p-r})]\{S_r\} + {}^{t}[\bar{B}(q_\bullet)][D] \sum_{r=1}^{p-1} \frac{1}{2}[A(q_{p-r})]\{\theta(q_r)\}\,dv \tag{32}$$

$$\{R_p^{\alpha}\} = -\int_v {}^{t}[B_\alpha][D] \sum_{r=1}^{p-1} \frac{1}{2}[A(q_{p-r})]\{\theta(q_r)\}\,dv \tag{33}$$

We can note that the matrix allowing to construct the tangent stiffness matrix are identical to those proposed by Büchter et al. and the new terms introduced here are $\{F_p^{nl}\}$ and $\{R_p^{\alpha}\}$ only.

3.4. Continuation procedure

The method presented before allows us to systematically compute a large number of terms of the series (8) and (9) which provides a quantitative description of the solution path in a large neighbourhood of the starting point. In the moderate rotation case ([5,15]), it has been established that the computational cost is equivalent to that of a modified Newton–Raphson step, i.e. an iteration with a constant stiffness matrix. However, the series generally have a finite radius of convergence. So, to describe the full solution path, the method should be applied in a step by step manner. At each step, the maximal value of the path parameter 'a' should be defined automatically by analysing the convergence of the power series. Cochelin [13] has proposed two ways of defining the range of validity of the series. The first one is based on the difference in the displacements at two successive orders which must be smaller than a given value ϵ_1.

$$\text{Validity range:} \quad a_{\max} = \left(\epsilon_1 \frac{\|u_1\|}{\|u_p\|} \right)^{1/p-1} \tag{34}$$

This way of evaluating the validity range is very simple, but it cannot guarantee a good residual at the end of the given step. A second validity range definition has been proposed. It is directly based on the residual vector whose increment must stay approximately below a given value ϵ_2 which is defined by the user. It is more convenient to consider a relative residual than the absolute one, which leads to the formula (Vannucci et al. [34])

$$\text{Validity range:} \quad a_{\max} = \left(\epsilon_2 \frac{\lambda \|F\|}{\|F^{nl}_{p+1}\|} \right)^{1/p+1} \tag{35}$$

One of the originalities of this method is that the step length is determined a posteriori, that is to say, it depends on the intrinsic characteristics of the computed series. Hence, by using this continuation procedure, the algorithm becomes automatic and the user operates easily. The validity range allows us to limit the asymptotic solution for each computed step at the end of which a residual is left and can become important after a number of steps. To avoid this growth of the residual, we correct the final solution by the standard Newton–Raphson process, if the relative residual is beyond a given value ϵ_3.

Thus, we have two criteria (34) and (35) to define the step length and the continuation algorithm depends on two accuracy parameters ϵ_1 (or ϵ_2) and on ϵ_3. Furthermore, the computation of a series depends on the order of truncature. In what follows, we shall discuss how to choose these parameters to optimize the efficiency of the algorithm.

3.5. Discussion and remarks

In this study, the solution branch of the nonlinear problem is obtained in a step by step manner. At each step, we determine an analytic expression of the branch under the form of the power series (8) and (9). More precisely, it is a discrete form of (8) and (9) which is actually computed since a finite element method is used to solve the continuous problems. The outputs of the program are in fact: the vectors q_p and α_p, i.e. the discrete form of the displacement field u and of the enhanced strain $\tilde{\gamma}$, and the corresponding stress S_p at the Gauss points. In other words, we compute an analytic representation of the solution branch of the finite element model.

To achieve the best efficiency, we have used a lot of different formulations and an obvious question is then: do all these choices of variables and formulations have an influence on the final results? The answer is definitely no, and the reasons why are underlined below:

- Once the path parameter is properly defined (here, the equation 10) the series representation (8) and (9) of the solution branch is unique.
- If in addition, the discretization of the structure is given (i.e. the mesh and the type of element), then, the discrete form of (8) and (9) is also unique.

Hence, the choice of the variables and of the formulation at each level has been guided by considerations of easiness and efficiency only. We have started with the three field Hu–Washizu principle in order to apply the EAS concept and to come to the formulation (5) with respect to u and $\tilde{\gamma}$. Next, we have reintroduced the stress to get a quadratic nonlinearity which permits a very simple expansion procedure (Section 3.1). Then, the three field linear problem (14) at order p has been transformed into the equilibrium and compatibility equations (18)

and (19) with respect to variables u_p and $\tilde{\gamma}_p$ only, the stress S_p being given by the constitutive law (16). Finally, a classical finite element method with condensation of the extra strain, on the element level, is used.

This approach is the most efficient way of computing the series at large orders of truncature. The reader who is doubtful about that, is invited to test other ways of proceeding, for instance:

(1) Starting with the equations of the problem written in strong form (local equation).
(2) Performing the expansion procedure and getting the linear problem at order p under the strong form.
(3) Making a weak Hu–Washizu formulation of the problem at order p.
(4) Applying the EAS concept to keep only u and $\tilde{\gamma}$ as variables.
(5) Applying the finite element method to solve the problem. The discrete equations (31) and (29) will be exactly found.

Another way could be:

(1) Starting with Hu–Washizu formulation and applying the EAS concept to achieve (5).
(2) Applying the finite element method to get an algebric nonlinear system of equations with respect to the vectors q and α.
(3) Expanding q and α with respect to the path parameter 'a', and forming the set of linear problems at each order with respect to u_p and $\tilde{\gamma}_p$.

Once again (31) will be exactly achieved, however with a more complex rhs vector because of the cubic nonlinearity with respect to q.

4. Applications

In this section, we validate the algorithm previously presented and we discuss the efficiency of the ANM as compared to incremental iterative algorithms.

The iterative method is considered as the numerical reference for the present study and is generally computed by the Abaqus code. This latter proposes an updated Lagrangian formulation, an iterative algorithm of Newton–Raphson with an arc length control parameter and an eight nodes quadrilateral element whose accuracy is similar to the shell element presented in this paper. Four problems will be considered:

(1) elastic buckling analysis of cylindrical shell with two rectangular cutouts,
(2) a cantilever beam loaded at its tip by a load of constant vertical direction,
(3) Lateral buckling of a cantilever beam,
(4) Point loaded hemispherical shell.

The first and the fourth examples are classical benchmarks, which have been studied by many authors. These four tests have been chosen to assess the capability of the algorithm to account for large rotations and to analyse bifurcation problems.

4.1. Buckling of a cylindrical shell with two holes

We consider a cylindrical shell with two diametrically opposed rectangular cutouts which are placed in the middle between the two ends (Fig. 2). It is subjected to a uniform axial compression [24,29]. Due to the symmetry of this set-up, only one octant of the structure will be considered in the computational model. It is discretized with three regular meshes involving, respectively, 504, 1830 and 10416 degrees of freedom and using the shell element presented in Section (3.3).

This example is studied to define the best strategy for the asymptotic numerical algorithm, but no comparison with iterative methods will be presented. The main parameter considered here is the order of truncature series. The typical response curve is pictured in Fig. 3 where the end of each step is indicated by a number. We have analysed a part of this curve, until the deflection, at the node located in the middle of vertical edge of the cutout, reaches a value of 10 mm, shortly after the maximal load point. For this first analysis, we have defined the step length by the displacement criterion (34) with accuracy parameters $\epsilon_1 = 10^{-5}$ and $\epsilon_3 = 10^{-3}$, but we do not need any correction phases to get a final relative residual below ϵ_3.

In Table 1, we present first the number of steps which are necessary to achieve the computation, second the ratio between the time to evaluate the rhs Fnl and the time $t1$ needed for evaluation and decomposition of the tangent stiffness matrix Kt, third the total relative time which is the ratio between the total CPU time and the

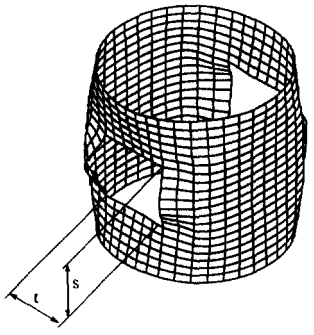

Geometry :
L = 200. mm
R = 100. mm
h = 1. mm
s = 80. mm
t = 79.5 mm

Material :
E = 71122.5 Mpa
v = 0.3

Fig. 2. Deformed configuration of cylindrical shell under axial and uniform pressure $P = 981.$ N/mm.

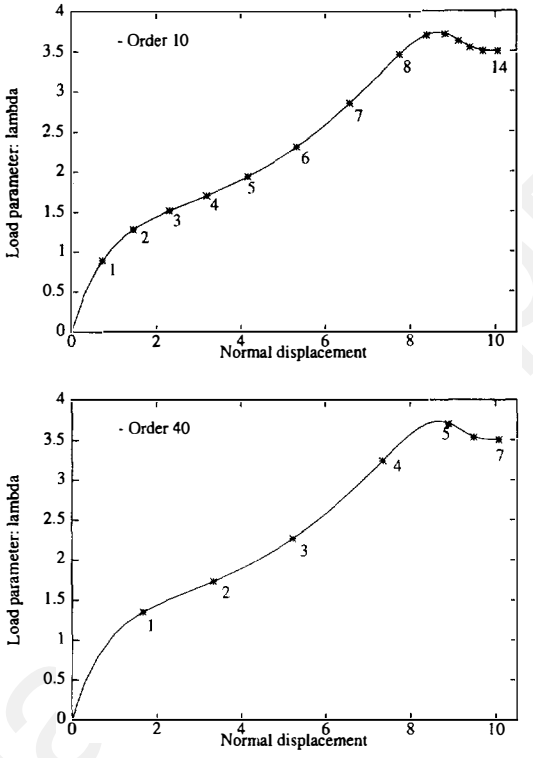

Fig. 3. ANM in continuation process for different orders.

Table 1
Buckling of cylindrical shell with two holes. Computing time in ANM (Computer used: HP 9000 K 200)

		Order 10	Order 15	Order 20	Order 30	Order 40
504 dof	Step number	8	6	6	5	5
	$\frac{Fnl\ evaluation}{Kt\ decomposition}$	0.50	0.84	1.24	2.23	3.46
	Total relative time	12.00	11.04	13.44	16.15	22.30
1830 dof	Step number	14	10	9	8	7
	$\frac{Fnl\ evaluation}{Kt\ decomposition}$	0.45	0.76	1.12	1.98	3.05
	Total relative time	20.30	17.60	19.08	23.84	28.35
10416 dof	Step number	14	10	9	8	7
	$\frac{Fnl\ evaluation}{Kt\ decomposition}$	0.39	0.64	0.94	1.68	2.58
	Total relative time	19.46	16.40	17.46	21.44	25.06

time $t1$. Roughly speaking, $t1$ is the time necessary to solve the corresponding linear elastic problem. For example, by considering the problem with 1830 d.o.f. at order 10, about half of Kt decomposition time is needed to evaluate the rhs vectors Fnl. So, for this example, the required computational time is equivalent to about 20 evaluations and decompositions of tangent stiffness matrix.

As expected, the number of steps decreases when the order of truncature increases. This phenomenon is significant, because we need twice as many steps at order 10 than at order 40. At order 10, most of the time is spent in the treatment of the stiffness matrix, the computation of the rhs requires 45% of the total running time with 1830 d.o.f. and only 39% with 10416 d.o.f. However higher orders involve a lot of Fnl evaluations, which become rather expansive. For this problem, the best compromise is obtained by using 15 terms of the series whatever be the size of the problem. One gets very close results with order 20, which has been found optimal in previous tests [15].

The results in Table 1 also establish that the ANM is more efficient for large scale problems. Indeed, the relative time to evaluate the r.h.s. at order 15 decreases about 25% from mesh with 504 d.o.f. to the one using 10416 d.o.f.($(0.84-0.64)/0.84 \simeq 0.25$).

Note that the number of steps is exactly the same with the two finest meshes. This is quite natural, because this number is representative of the nonlinearity of the response curve, that very little changes with the mesh. The case of the sparest mesh is very different, because it is not sufficient to correctly represent the physical problem and because it yields a stiffer response than the two other ones. Also note that the total time at order 20 with 1830 and 10416 d.o.f. is respectively about 12 mn and 90 mn.

4.2. Flexion of a beam

Geometrically nonlinear analysis of a cantilever beam is considered in this example which involves finite rotations. The beam described in Fig. 4, is loaded at its tip by a force with constant vertical direction.

This problem has been treated by Newton–Raphson algorithm with different strategies. To obtain a deflection of 9 mm at the loaded point, Abaqus code requires 26 steps and a total of 94 stiffness matrix decompositions when it is used with an adaptative arc length and a maximum relative residual of 5×10^{-3} allowed for each step. By using a constant arc length parameter 's' with different values, this algorithm requires 110 decompositions for $s = 1$ and 26 decompositions when $s = 10$, but in this last case, we only obtain five discrete points for the whole solution path.

This problem, when solved by ANM, gives spectacular results. Indeed, with only one stiffness matrix decomposition, we obtain the exact solution branch up to a deflection of 8 mm (see Fig. 4). A more accurate analysis can be done from the curve of the residual in Fig. 5. For instance, if we require an accuracy of $\epsilon_3 = 10^{-3}$, the first step allows us to reach a deflection of about respectively 6, 7 or 8 mm for an order of truncature of 20, 30 or 100. One can also remark that the step length is 2.5 times larger at order 20 than at order 8, which explains the interest of choosing sufficiently large order of truncature series. When the continuation procedure is used with order 20 and $\epsilon_1 = 10^{-5}$ and $\epsilon_3 = 10^{-3}$, two steps are necessary to describe the whole solution branch without correction phases needed.

4.3. Lateral buckling of a cantilever beam

In this example, we consider the Prandtl buckling of a cantilever beam described in Fig. 6. For discretization, we use a regular mesh with 510 degrees of freedom and 20 elements. The geometry of the structure is slightly perturbed in order to avoid the pure bifurcation case and to have a continuous equilibrium path with a quasi-bifurcation. The calculation made with Abaqus code using an adaptative step of Riks method and a maximum residual allowed of 5.10^{-3} requires 50 steps and a total of 223 decompositions of the tangent stiffness matrix to reach a displacement U2 of 70 mm at the loaded point. The same calculation has been realised by the

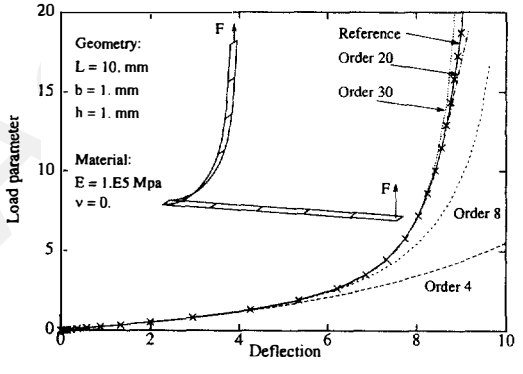

Fig. 4. Load/deflection diagram, of the loaded point, for different orders of truncature series. Only one computation step has been done.

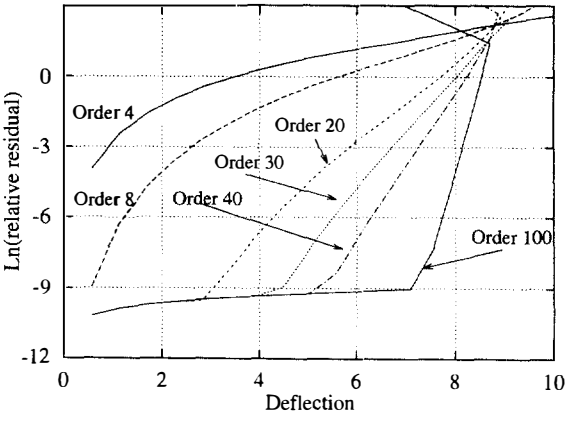

Fig. 5. Logarithm of relative residual force/deflection diagram for different orders of truncature.

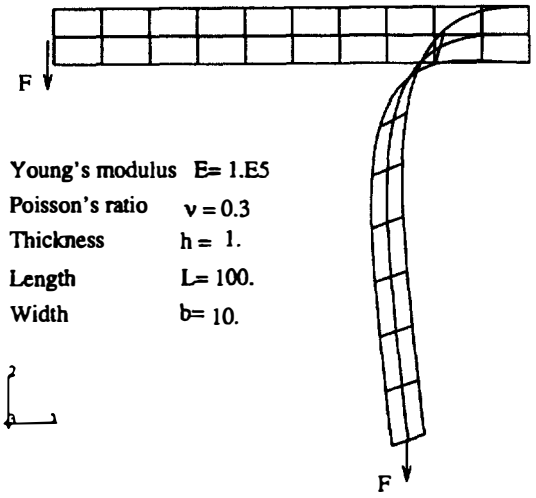

Fig. 6. Initial and deformed configurations of the cantilever. The initial geometry is perturbed by an initial imperfection whose maximal value is h/10. and whose shape is given by the first buckling mode.

ANM at order 20, using a smaller relative residual $\epsilon_3 = 10^{-3}$ and an accuracy parameter based on displacement criterion $\epsilon_1 = 10^{-5}$. The computation requires only12 steps to describe the whole solution branch. Figs. 7 and 8 describe the equilibrium path: continuous curves represent the Abaqus reference solution and the crosses represent the ends of each ANM step. We can distinguish three fields: a linear pre-buckling branch, the switch to the bifurcating branch, and the post-buckling range, where large rotations occur.

The ABAQUS code requires 32 steps to describe the sudden change of the solution at the bifurcation, i.e. u_2 is 5 mm after 32 steps, and 18 more steps for the post-buckling branch until the loaded node reaches a deflection of 70 mm. However, when ANM is used, the computation requires only 8 steps for the first part of the branch and 4 steps to describe the nonlinear branch left.

Furthermore, we have done a comparative study using the displacement criterion (34) and the residual one (35). We have limited the troncature series at order 15 (optimal order in the first example). Results of this study are reported on Table 2: for each criterion, we give logarithm of relative residual and the step number in respect to imposed accuracy. We remark that the two criteria (34) and (35) can be considered as more or less equivalent provided the parameter ϵ_1 or ϵ_2 is suitably chosen. More precisely, the parameter ϵ_1 must be sufficiently small (i.e. less than 10^{-4}) and on the contrary, the parameter ϵ_2 mustn't be too large (i.e. less than 10^{-1}) in order to limit the number of steps with a good final residual. We also remark that, in the two cases, to obtain a final residual of about 10^{-4}, 12 steps are required, and to obtain a final residual of 10^{-6}, about 18 steps are necessary. This example allows us to confirm the high-quality of the ANM and its capability to deal with large rotations as

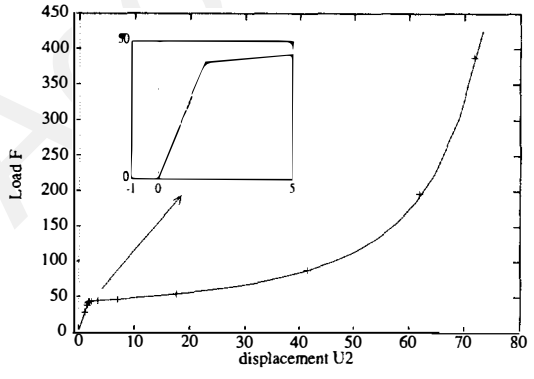

Fig. 7. Load/displacement U2 diagram for the loaded node.

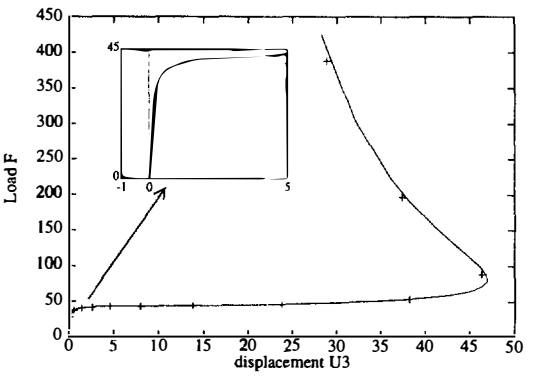

Fig. 8. Load/displacement U3 diagram for the loaded node.

Table 2
Lateral buckling of a cantilever beam. Comparison between criteria based on displacement and residual in ANM

Displacement criterion	Accuracy	10^{-7}	10^{-6}	10^{-5}	10^{-4}	10^{-3}
	Final residual (log10)	−5.9	−5.9	−5.0	−3.9	−2.8
	Steps number	19	17	14	12	10
Residual criterion	Accuracy	10^{-4}	10^{-3}	10^{-2}	10^{-1}	1
	Final residual (log10)	−5.5	−5.4	−4.8	−3.7	−2.8
	Steps number	18	16	14	12	10

well as with bifurcation points. Furthermore, it is able to define automatically an adaptative step length by evaluating the local nonlinearity of the response curve.

4.4. Point loaded hemispherical shell

In this example, we present the famous benchmark of a hemispherical shell with an 18^0 hole, loaded by pinching forces ($F = 1.$) as shown in Figs. 9 and 10. Due to the problem symmetry, we discretize only a quarter

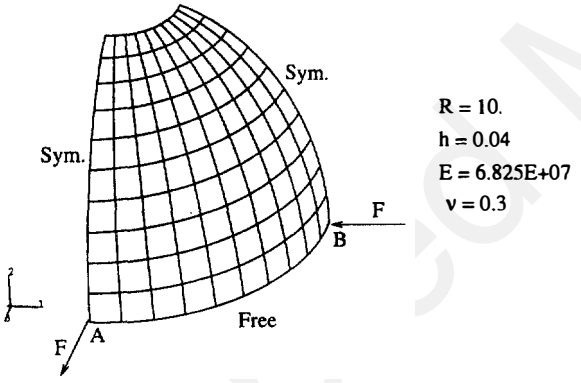

Fig. 9. Geometry description for pinched hemisphere.

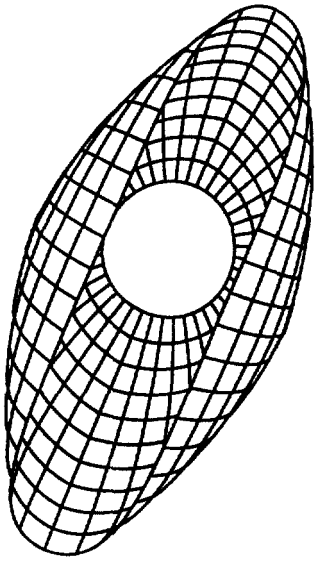

Fig. 10. Pinched hemisphere in deformed state.

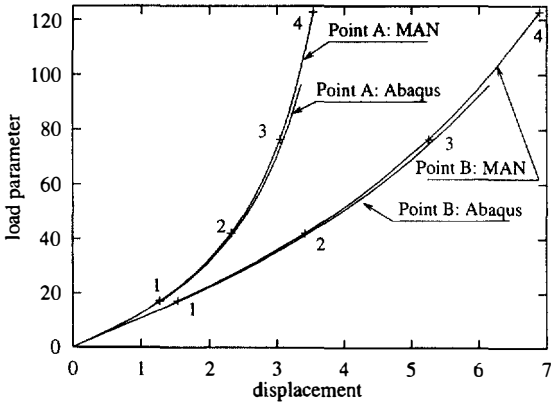

Fig. 11. Pinched hemisphere: load-deflection path in which the computed range of validity is based on the displacement criterion.

of the structure using a regular mesh with 2166 degrees of freedom and 108 elements. This problem was already studied by Saleeb [30], Büchter et al. [10] and Ammar [1].

The load-deflection path is presented in Fig. 11. By using asymptotic numerical algorithm based on displacement criterion, $\epsilon_1 = 10^{-6}$ and $\epsilon_3 = 10^{-3}$, only 4 steps are needed to reach a deflection of 6 mm. However, the same problem requires 104 tangent stiffness matrix when Abaqus code is used with Riks method and with an adaptative step length ($\epsilon_3 = 5 \times 10^{-3}$).

The conclusions are similar to the ones obtained for the previous examples, with a great advantage for ANM in the present case.

5. Conclusion

In this work, the Asymptotic Numerical Method has been developed to analyse large rotations of elastic shells. The theoretical formulation and the finite element discretization have been chosen in such a way that we have been able to use the same simple algorithm as within the moderate rotation framework. In some cases, we have found very large step lengths. This result is not completely surprising because the development of large deformations is generally considered as a much less penalizing nonlinearity than unilateral contact, friction or plastic behaviour. By considering the results of this paper, the ANM appears much more efficient than the classical incremental methods for applications to large rotations of elastic shells.

Once more, the ANM algorithm proved very robust, which has allowed us to get solution paths, that are very close to a bifurcation point (see [33] for other illustrations). It would be straightforward to include in our code some algorithms to detect bifurcation points [8] or to compute bifurcating branches [34].

We have also discussed the optimal characteristics of the ANM algorithm. Contrary to many previous works, we have included the possibility of iterative corrections at the end of each step, in order to limit the growth of the residual vector (see [34] for other examples), but for all exemples presented in this study, no correction phases are needed when we use a sufficiently small parameter ϵ. As within moderate rotations, the optimal order of truncature is large and nearly equal to 20, which contributes to the efficiency of the algorithm. Likely, this interesting feature is strongly connected to our choice of a simple theoretical formulation and of the associated finite element.

It will be also interesting to compare our numerical procedure with the one of Ammar [1], which is based on a different formulation, a different element and an alternative way of computing the series. Notice that the element proposed by Büchter et al. [11] is well adapted to account for plasticity. Finally, it seems possible to establish similar algorithms for finite rotations of beams [3,22].

Appendix A

$$[R] = \begin{bmatrix} g_1^x & g_1^y & g_1^z & 0 & 0 & 0 & 0 & 0 & 0 \\ 0 & 0 & 0 & g_2^x & g_2^y & g_2^z & 0 & 0 & 0 \\ 0 & 0 & 0 & 0 & 0 & 0 & g_3^x & g_3^y & g_3^z \\ g_2^x & g_2^y & g_2^z & g_1^x & g_1^y & g_1^z & 0 & 0 & 0 \\ 0 & 0 & 0 & g_3^x & g_3^y & g_3^z & g_2^x & g_2^y & g_2^z \\ g_3^x & g_3^y & g_3^z & 0 & 0 & 0 & g_1^x & g_1^y & g_1^z \end{bmatrix}$$

References

[1] S. Ammar, Méthode asymptotique numérique perturbée appliquée à la résolution des problémes non linéaires en grande rotation et grand déplacement, Thesis, Université Laval Québec, Faculté des sciences etde génie, 1996.

[2] J. Argyris, An excursion into large rotations, Comput. Methods Appl. Mech. Engrg. 32 (1982) 85–155.

[3] J.H. Argyris and Sp. Symeonidis, Nonlinear finite element analysis of elastic systems under nonconservative loading-natural formulation. Part I. Quasistatic problems, Comput. Methods Appl. Mech. Engrg. 26 (1981) 75–123.
[4] S.N. Atluri and A. Cazzani, Rotations in computational solid mechanics, Arch. Comput. Methods Engrg. 2(1) (1995) 49–138.
[5] L. Azrar, B. Cochelin, N. Damil and M. Potier-Ferry, An asymptotic-numerical method to compute the post-buckling behaviour of elastic plates and shells, Int. J. Numer. Methods Engrg. 36 (1993) 1251–1277.
[6] Y. Basar and Y. Ding, Finite rotation elements for the nonlinear analysis of thin shell structures, Int. J. Solids Struct. 26 (1990) 83–97.
[7] H. De Boer and F. Van Keulen, Padé approximants applied to a nonlinear finite element solution strategy, in: Numerical Methods in Engineering 96 (1996) 171–176, Proceedings of the Second ECCOMAS Conference on Numerical Methods in Engineering, 9–13 September 1996, Paris, France.
[8] E.H. Boutyour, B. Cochelin and M. Potier-Ferry, Calculs des points de bifurcation par une méthode asymptotique numérique, in: Proceedings 1st Congrés National de Mécanique au Maroc (1993) 371–378.
[9] B. Braikat, N. Damil and M. Potier-Ferry, Méthodes asymptotiques numériques pour la plasticité, Revue Européenne des Éléments Finis 6(3) (1997) 337–357.
[10] N. Büchter and E. Ramm, Shell theory versus degeneration—a comparison in large rotation finite element analysis, Int. J. Numer. Methods Engrg. 34 (1992) 39–59.
[11] N. Büchter, E. Ramm and D. Roehl, Three dimensional extension of non-linear shell formulation based on the enhanced assumed strain concept, Int. J. Numer. Methods Engrg. 37 (1994) 2551–2568.
[12] J.M. Cadou, B. Cochelin and M. Potier-Ferry, The asymptotic numerical method application to fluid-structure interaction, in: Computational Fluid Dynamics 96 (1996) 131–138, Proceedings of the Third ECCOMAS Computational Fluid Dynamics Conference, 9–13 September 1996, Paris, France.
[13] B. Cochelin, Méthode asymptotique-numérique pour le calcul non-linéaire géométrique des structures élastiques, Habilitation á diriger des recherches, Université de Metz 1994.
[14] B. Cochelin, A path-following technique via an asymptotic-numerical method, Comput. Struct. 53(5) (1994) 1181–1192.
[15] B. Cochelin, N. Damil and M. Potier-Ferry, The asymptotic-numerical method: an efficient perturbation technique for non-linear structural mechanics, Revue Européenne des Éléments Finis 3(2) (1994) 281–297.
[16] N. Damil and M. Potier-Ferry, A new method to compute perturbed bifurcation Application to the buckling of imperfect elastic structures, Int. J. Engrg. Sci. 26(9) (1990) 943–957.
[17] M. Potier Ferry, N. Damil, B. Braikat, J. Descamps, J.M. Cadou, H.L. Cao and A. Elhage Hussein. Traitement des fortes non-linéarités par la méthode asymptotique numérique. C.R. Acad. Sci. Paris, t.324, Série II b (1997) 171–177.
[18] R.H. Gallagher, Perturbation procedures in nonlinear finite element structural analysis, Computational Mechanics—Lecture Notes in Mathematics 75–89 (Springer–Verlag, Berlin 1995) 461.
[19] M. Geradin and D. Rixen, Parametrization of finite rotations in computational dynamics a review, Revue Européenne des Éléments Finis 4(5–6) (1995) 497–553.
[20] S. Hadji, Méthode de résolution pour les fluides incompressibles, Thesis, Université de Technologie de Compiégne, 1995.
[21] A. Ibrahimbegovic, Finite elastic deformations and finite rotations of 3d continuum with independent rotation field, Revue Européenne des Éléments Finis 4(5–6) (1995) 555–576.
[22] A. Ibrahimbegovic, H. Shakourzadeh, J.L. Batoz, Mazen Al Mikdad and Y.Q. Guo, On the role of geometrically exact and second order theories in buckling and post-buckling analysis of three-dimensional beam structures, Comput. Struct. 61(6) (1996) 1101–1114.
[23] A. Najah, B. Cochelin, N. Damil and M. Potier-Ferry, A critical review of asymptotic numerical methods, Arch. Comput. Methods Engrg. 5(1) (1998) 31–50.
[24] A.K. Noor, Recent advances in reduction methods for nonlinear problems, Comput. Struct. 13 (1981) 31–44.
[25] A.K. Noor and J.M. Peters, Reduced basis technique for nonlinear analysis of structures, AIAA J. 18(4) (1980) Article No. 79-0747R.
[26] A.K. Noor and J.M. Peters, Tracing post-limit-point paths with reduced basis technique, Comput. Methods Appl. Mech. Engrg. 28 (1981) 217–240.
[27] W. Pietraszkiewicz, Lagrangian description and incremental formulation in the non-linear theory of thin shells, Int. J. Non-Linear Mech. 19(2) (1983) 115–140.
[28] W. Pietraszkiewicz and J. Badur, Finite rotations in the description of continuum deformation, Int. J. Engrg. Sci 21 (1983) 1097–1115.
[29] E. Riks, Some computational aspects of the stability analysis of nonlinear structures, Comput. Methods Appl. Mech. Engrg. 47 (1984) 219–259.
[30] A.F. Saleeb, T.Y. Chang and W. Graf, A quadrilateral shell element using a mixed formulation, Comput. Struct. 26(5) (1987) 787–803.
[31] J.C. Simo and M.S. Rifai, A class of mixed assumed strain methods and method of incompatible modes, Int. J. Numer. Methods Engrg. 37 (1990) 1595–1636.
[32] J.M.T. Thompson and A.C. Walker, The non-linear perturbation analysis of discrete structural systems, Int. J. Solids Struct. 4 (1968) 757–768.
[33] A. Tri, B. Cochelin and M. Potier-Ferry, Résolution des équations de Navier–Stokes et détectiondes bifurcations stationnaires par une méthode asymptotique numérique, Revue européenne des éléments finis 5(4) (1996) 415–442.
[34] P. Vannucci, B. Cochelin, N. Damil and M. Potier-Ferry, An asymptotic numerical method to compute bifurcating branches, Int. J. Numer. Methods Engrg. 41 (1998) 1365–1389.
[35] O.C. Zienkiewicz and R.L. Taylor, The Finite Element Method, 4th ed. (McGraw-Hill Book Company, 1991).